International Journal of Engineering Research & Technology (IJERT)
ISSN: 2278-0181
Vol. 8 Issue 05, May-2019

Study of effect of Gurney Flap on an inverted NACA 23012 Rear Wing

Krishna Ganesan [1] Sai Gowtham J [2]
1 & 2, Independent Researchers
Chennai, India

***Abstract*— This research paper aims to study the effect of attaching a Gurney flap on the trailing edge of an inverted NACA 23012 rear wing. The model was created in AutoCAD 2013, and the mesh was defined in the pre-processing software ANSYS Gambit 2.4.6. The flow analyses were done considering the rear wing to be placed in a pressure far field without considering the ground effect. The results were plotted for various factors like downforce, drag and the downforce to drag (L/D) ratio for various heights of the Gurney flap. A velocity inlet model for an air speed of 0.1 Mach (33 m/s) was chosen and the analyses were iterated with different angles of attack. The standard two-equation turbulence kinetic energy and turbulence dissipation model was chosen for the solver. The numerical analysis was carried out in ANSYS Fluent 14.5. The contours of pressure distribution, pressure coefficient and the flow path lines generated were visualized for varying flow characteristics within the computational domain. It was observed that the downforce to drag (L/D) ratio increases with an increase in the angle of attack and the Gurney height.**

Keywords—Race car aerodynamics; Gurney flap; downforce; Computational Fluid Dynamics (CFD)

I. INTRODUCTION

Automotive aerodynamics, deals with the study of interaction between the fluid stream around the automobile and aims to reduce the drag, wind noise, preventing undesired lift and other causes of aerodynamic instability at high speeds. For some classes of racing vehicles, it is important to produce downforce to improve traction and thus enhancing their cornering abilities. The widely used automotive aerodynamic component to generate the required downforce is a rear wing, which is an inverted airfoil. Since the principles of aerodynamics conform to automotive applications as well, their governing laws and principles can be applied for racecar aerodynamics as well. It can be noted that, although the rear wing produces significant downforce, it is almost constant. To overcome this, the profile has to be modified, meaning, that the camber, chord, leading and trailing edge profiles has to be redesigned. Interestingly, the downforce, a rear wing produces can be increased without the need of complex redesigning, by attaching a Gurney flap at the trailing edge of the rear wing with a variable angle of attack spoiler. In this research paper, we have investigated the effect of attaching a Gurney flap on the trailing edge of a NACA 23012 rear wing and studying its effects by varying the angles of attack within the computational domain.

II. SYSTEM DEFINITIONS

A. Spoiler (Rear Wing)

A spoiler is an automotive aerodynamic device whose intended function is to 'spoil' the unfavorable air movement across the body of a vehicle. A spoiler diffuses air by increasing the amount of turbulent air flowing over it, 'spoiling' the laminar flow and providing a cushion for the laminar boundary layer. A spoiler's shape can be defined by its cross section, which is an inverted airfoil, and generates a negative lift called downforce. A race car at much higher speeds (air velocity ≥ 25 m/s), tends to lose its tractive adhesion to the track owing to the tremendous amount of lift being generated beneath it, because of the volume of the air flow over and under the chassis. Spoilers are used in the front, in the form of front wings as well as in the rear of the car to generate more downforce. This downforce is necessary in maintaining high speeds through the corners and enables the car to remain on the track.

B. Airfoil Terminology

The suction surface is generally associated with higher velocity and lower static pressure. The pressure surface has a higher static pressure. The pressure gradient between these two surfaces contributes to the lift force for a given airfoil.

A key characteristic of an airfoil is its chord. We thus define the following concepts:

(a) The leading edge is the point at the front of the airfoil with maximum curvature.

(b) The trailing edge is the point of minimum curvature at the rear end of the airfoil.

(c) The chord line is a straight line connecting the leading and trailing edge.

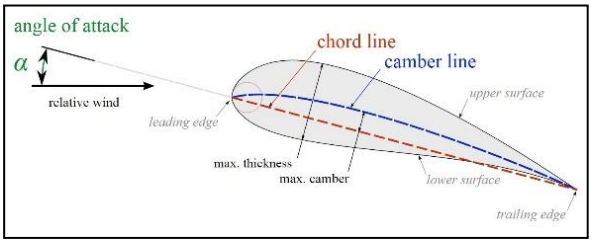

Figure 1 - Airfoil Nomenclature [1]

C. NACA Airfoil

The National Advisory Committee for Aeronautics (NACA) was a U.S. federal agency for aeronautical research. Of the many airfoils that NACA has designated, NACA four digit series and five digit series are widely used. For this

International Journal of Engineering Research & Technology (IJERT)
ISSN: 2278-0181
Vol. 8 Issue 05, May-2019

research, we have selected a NACA 23012, as it is the widely used airfoil profile in automotive racing and other automotive aerodynamic applications. The design parameters of NACA 23012 are

(a) Maximum camber is 1.8% chord
(b) Maximum thickness is 12% chord
(c) Maximum camber occurs at 12.7% chord
(d) Maximum thickness occurs at 29.8% chord
(e) Maximum designed coefficient of lift is 0.3

D. Gurney Flap

The Gurney Flap is a small flat tab projecting from the trailing edge of the rear wing. Typically set at a right angle to the pressure surface of the airfoil. This improves the performance of a simple airfoil to the same level as a complex high-performance design. It operates by increasing the pressure on the pressure side and decreasing it on the suction side, and helping the boundary layer flow to stay attached all the way to the trailing edge [4]. The original application, developed by Dan Gurney was a right-angled piece of sheet metal, fixed to the top trailing edge of the rear wing of his racing car. The device was installed pointing upwards to increase downforce, and thus improving traction. He tested it and found that it allowed his car to negotiate turns at higher speed, while also achieving higher speed in the straight sections. The flap increases the maximum lift coefficient, decreases the angle of attack, which is consistent with an increase in camber of the airfoil. The Gurney flap increases lift by altering the Kutta condition (A body with a sharp trailing edge, which is moving through a fluid, will create about itself a circulation of sufficient strength to hold the rear stagnation point at the trailing edge). The wake behind the flap is a pair of counter-rotating vortices that are alternately shed in a von Kármán vortex street (It is a repeating pattern of swirling vortices caused by the unsteady separation of flow of a fluid around blunt bodies) [5]. The increased pressure on the surface ahead of the flap means the upper surface suction can be reduced while producing the same lift.

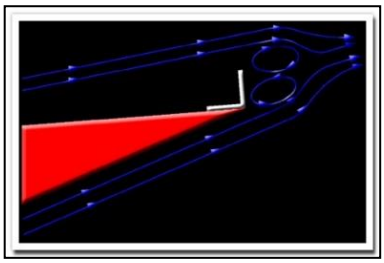

Figure 2 - Gurney Flap with vortex formation [2]

III. GOVERNING EQUATIONS

A. Bernoulli's Principle

It states that for an inviscid flow, an increase in the speed of the fluid occurs simultaneously with a decrease in pressure or a decrease in the fluid's potential energy. For a fluid, the potential energy is represented by the static pressure (P_s). The kinetic energy is a function of the motion of the air, and it's mass. The sum of both static pressure and dynamic pressure is a constant.

$$P_s + \tfrac{1}{2}\rho V^2 = K \qquad (1)$$

Equation (1) represents the Bernoulli's principle.

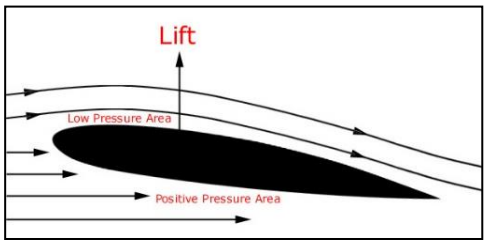

Figure 3 - Flow pattern around an airfoil [3]

B. Continuity Equation

It says that the density, velocity and the area that enters the system is always equal to the density, velocity and the area that leaves the system. It conforms to the law of conservation of mass.

$$\rho_1 A_1 V_1 = \rho_2 A_2 V_2 \qquad (2)$$

Equation (2) represents the Continuity Equation.

C. Navier Stoke's Equation

It describes the motion of fluid substances. It arises by applying Newton's second law to fluid motion, together with the assumption that the stresses in the fluid is the sum of a diffusing viscous term and a pressure term, hence describing a viscous flow. The Navier - Stoke's equations in their full and simplified forms help with the design of aircraft and cars.

$$\frac{\partial u}{\partial x} + \frac{\partial v}{\partial y} = 0 \qquad (3)$$

Equation (3) represents the Continuity in Navier - Stoke's Equation.

$$u\frac{\partial u}{\partial x} + v\frac{\partial u}{\partial y} = -\frac{1}{\rho}\frac{\partial p}{\partial x} + v\left[\frac{\partial^2 u}{\partial x^2} + \frac{\partial^2 u}{\partial y^2}\right] \qquad (4)$$

Equation (4) represents the X component in Navier - Stoke's Equation.

$$u\frac{\partial v}{\partial x} + v\frac{\partial v}{\partial y} = -\frac{1}{\rho}\frac{\partial p}{\partial y} + v\left[\frac{\partial^2 v}{\partial x^2} + \frac{\partial^2 v}{\partial y^2}\right] \qquad (5)$$

Equation (5) represents the Y component in Navier - Stoke's Equation.

D. Incompressible Flow

The question of whether the density of air flowing around a rear wing will change or not is crucial in aerodynamics. The molecules move to maintain a constant air density. This will only be possible if the flow is at a speed well below the speed of sound. Thus, if the velocities involved are below the speed of sound, the flow can be assumed as an incompressible one, as the changes in density, temperature and pressure are negligible. So the working of the rear wing can be most accurately described by considering the flow around it to be incompressible. As a result, when the velocity increases, the static pressure decreases.

International Journal of Engineering Research & Technology (IJERT)
ISSN: 2278-0181
Vol. 8 Issue 05, May-2019

IV. RESEARCH METHODOLOGY

In any research approach, it can be seen that there must be a scientific, systematic and iterative approach to arrive at the desired result based on a literature [6]. The two dimensional geometry of the airfoil was generated using a modeling software. It was meshed in a pre-processor and analyzed in a solver. The consistencies of the mesh files were checked and were refined iteratively when the desired result was not achieved. Similarly, the turbulence closure of the solver was adapted when the desired results were not achieved. The convergence of the residual plot was checked for each of the test cases and the analyses was considered valid only when the convergence was achieved properly without any errors. The results of the various analyses were inferred and a plot comparing the downforce with various angle of attack (α) and for various Gurney heights (H_g) were plotted. In addition to that, the drag force experienced and the downforce ro drag (L/D) ratio were observed for the various angles of attack (α). By comparing the data from all the analyses, the optimum Gurney height and the angle of attack was selected

.

V. MODELLING

The coordinates of the NACA 23012 airfoil are as given below. However, the signs were inverted to make the airfoil a rear wing.

TABLE 1 - COORDINATES OF NACA 23012 AIRFOIL

X	Y	X	Y
1.0000	0.0000	0.0030	-0.0055
0.9988	0.0002	0.0082	-0.0101
0.9952	0.0008	0.0156	-0.0140
0.9891	0.0018	0.0249	-0.0172
0.9807	0.0031	0.0362	-0.0199
0.9700	0.0049	0.0492	-0.0224
0.9569	0.0069	0.0639	-0.0246
0.9417	0.0093	0.0804	-0.0268
0.9243	0.0120	0.0987	-0.0290
0.9048	0.0149	0.1188	-0.0313
0.8834	0.0181	0.1408	-0.0338
0.8601	0.0214	0.1648	-0.0363
0.8351	0.0249	0.1910	-0.0387
0.8084	0.0286	0.2191	-0.0408
0.7802	0.0324	0.2487	-0.0424
0.7507	0.0362	0.2795	-0.0436
0.7200	0.0401	0.3114	-0.0443
0.6881	0.0439	0.3442	-0.0446
0.6554	0.0478	0.3777	-0.0445
0.6219	0.0515	0.4119	-0.0440
0.5879	0.0551	0.4465	-0.0431
0.5534	0.0586	0.4814	-0.0419
0.5186	0.0619	0.5163	-0.0404
0.4837	0.0649	0.5512	-0.0387
0.4490	0.0676	0.5858	-0.0368
0.4145	0.0700	0.6200	-0.0347
0.3803	0.0720	0.6536	-0.0324
0.3468	0.0737	0.6865	-0.0300
0.3140	0.0748	0.7184	-0.0276
0.2821	0.0755	0.7493	-0.0251
0.2513	0.0757	0.7790	-0.0226
0.2217	0.0754	0.8073	-0.0201
0.1934	0.0746	0.8341	-0.0176
0.1660	0.0731	0.8592	-0.0152
0.1399	0.0707	0.8827	-0.0129
0.1152	0.0672	0.9042	-0.0107
0.0923	0.0626	0.9238	-0.0086
0.0715	0.0570	0.9413	-0.0067
0.0531	0.0504	0.9566	-0.0050
0.0373	0.0432	0.9697	-0.0035
0.0241	0.0356	0.9805	-0.0023
0.0138	0.0279	0.9890	-0.0013
0.0063	0.0203	0.9951	-0.0006
0.0015	0.0130	0.9988	-0.0001
-0.0006	0.0062	1.0000	0.0000
0.0000	0.0000		

The design of the spoiler was done using AutoCAD 2013. A two dimensional geometry of the inverted airfoil was created using SPLINE and a C grid was drawn over the airfoil surface, such that it conforms to the mapping of both the upper and the lower surface geometries for the ease of meshing. The coordinate files were used to map the airfoil's coordinates and the Gurney flap was drawn as a separate component.

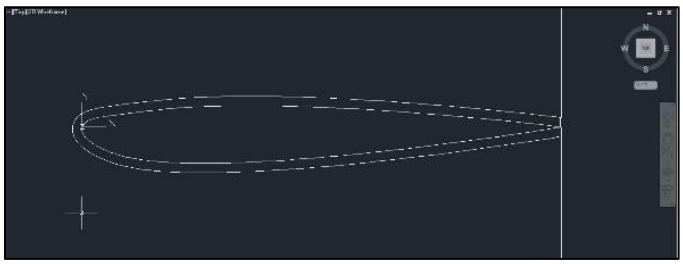

Figure 4 - NACA 23012-airfoil profile visualized in AutoCAD 2013

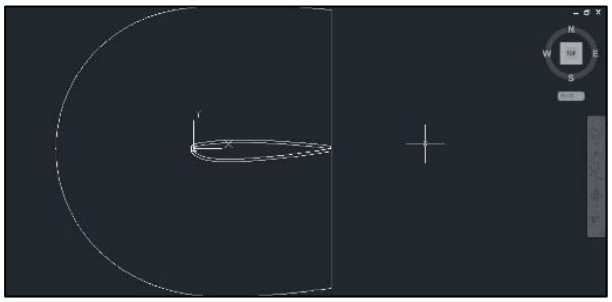

Figure 5 - NACA 23012-airfoil profile with C grid (computational domain)

VI. PRE - PROCESSING, SOLVER AND POST - PROCESSING

A. Pre - Processing

1) Grid Creation

The drawing file was imported into ANSYS Gambit 2.4.6 and the meshes were created such that they conform to the mapping, i.e., at any given point along the surface of the profile, the mesh lines are perpendicular. During initial meshing, several lines were skewed and on refining the mesh, it was rectified and the desired mesh was obtained. The rectangular blocks were created around the rear wing.

International Journal of Engineering Research & Technology (IJERT)
ISSN: 2278-0181
Vol. 8 Issue 05, May-2019

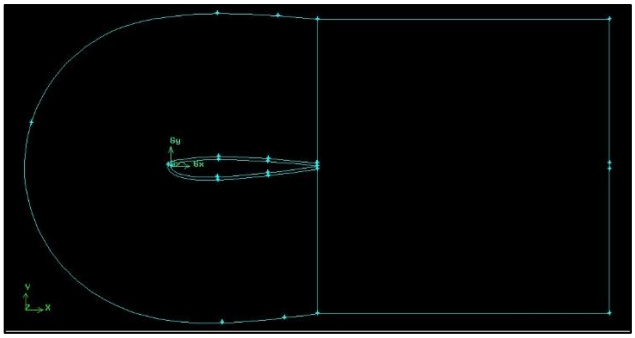

Figure 6 - Entire block visualized in the pre - processor

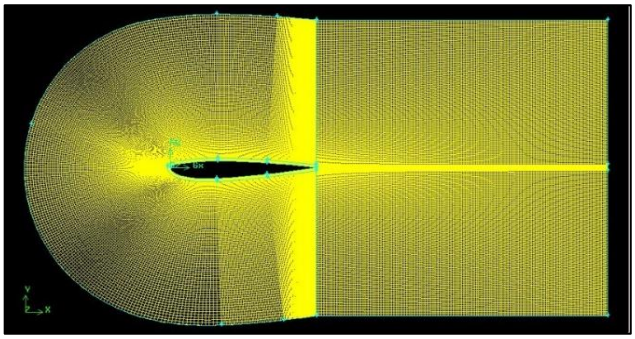

Figure 7 - Entire block visualized along with the mesh

2) Writing Mesh Files

After the required meshes were created, they were written as mesh files, so that they become compatible with the solver. The mesh files for Gurney heights 0%, 0.5%, 1%, 1.5% and 2% are shown below. The finer meshes near the surface for a better simulation results are to be noted here.

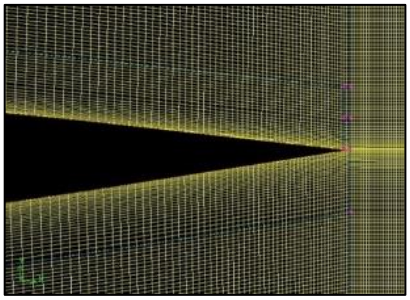

Figure 8 - Mesh for Gurney Height (H_g) = 0.0% of total chord length

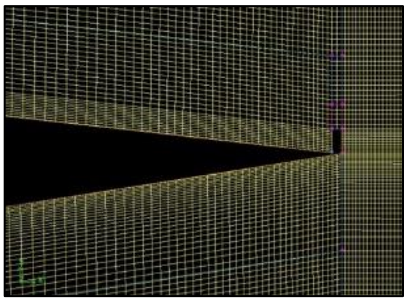

Figure 9 - Mesh for Gurney Height (H_g) = 0.5% of total chord length

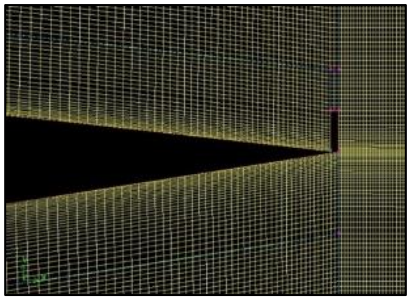

Figure 10 - Mesh for Gurney Height (H_g) = 1.0% of total chord length

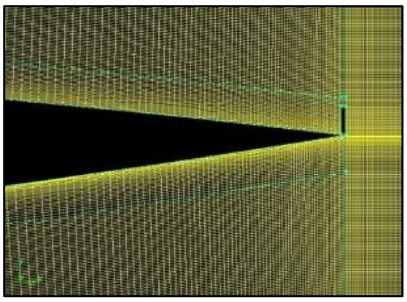

Figure 11 - Mesh for Gurney Height (H_g) = 1.5% of total chord length

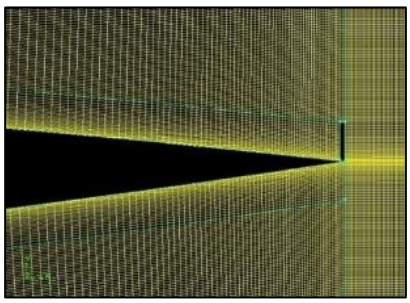

Figure 12 - Mesh for Gurney Height (Hg) = 2.0% of total chord length

B. Solver

ANSYS Fluent 14.5 was used for solving the simulation. Higher processing cores and man-hours were required to simulate this complex interaction of liquids and gases with surfaces which were defined by the boundary conditions. With high-speed parallel computing, and utilizing multi-cores, better simulation solutions were achieved.

1) Turbulence Modeling

Turbulence modeling is the construction and use of a turbulence model to predict the effects of turbulence in a computational domain. Averaging is often used to simplify the solutions of the governing equations, but models are needed to represent scales of the flow that are not resolved. Here we choose the widely used standard two-equation k-ε turbulence model. It is the most common model used in CFD analysis to simulate turbulent conditions. It is a two-equation model, which gives a general description of turbulence by means of two transport equations. The first transported variable determines the energy in the turbulence and is the turbulence kinetic energy (k). The second transported variable is the turbulence dissipation (ε) which determines the rate of dissipation of the turbulence kinetic energy [7]. For turbulence kinetic energy (k),

International Journal of Engineering Research & Technology (IJERT)
ISSN: 2278-0181
Vol. 8 Issue 05, May-2019

$$\frac{\partial(\rho k)}{\partial t} + \frac{\partial(\rho k u_i)}{\partial x_i} = \frac{\partial}{\partial x_j}\left[\frac{\mu_t}{\sigma_k}\frac{\partial k}{\partial x_j}\right] + 2\mu_t E_{ij}E_{ij} - \rho\epsilon \quad (6)$$

Equation (6) represents the Turbulence Kinetic Energy (k).

For turbulence dissipation (ε),

$$\frac{\partial(\rho\epsilon)}{\partial t} + \frac{\partial(\rho\epsilon u_i)}{\partial x_i} = \frac{\partial}{\partial x_j}\left[\frac{\mu_t}{\sigma_\epsilon}\frac{\partial \epsilon}{\partial x_j}\right] + C_{1\epsilon}\frac{\epsilon}{k}2\mu_t E_{ij}E_{ij} - C_{2\epsilon}\rho\frac{\epsilon^2}{k} \quad (7)$$

Equation (7) represents the Turbulence Dissipation (ε).

Where,

t = Time, p = Pressure, μ = Dynamic Viscosity
u_i = Velocity component in corresponding direction
E_{ij} = Component of rate of deformation
μ_t = Eddy viscosity
$C_\mu = 0.09$, $\sigma_k = 1.00$, $\sigma_e = 1.30$
$C_{1e} = 1.44$, $C_{2e} = 1.92$

2) Boundary Condition

The airfoil was considered to be placed in a free stream of air i.e. a pressure far field without considering the ground effect. The negative angle of attack specified in the table implies that the free stream of air comes from above the leading edge, as this is an inverted airfoil. A velocity inlet solver was chosen for analysis and an inlet velocity of 0.1 Mach (33 m/s) was specified. Air was chosen as standard material. The sine and cosine values resolved for the various angles of attack are represented in the table below.

TABLE 2 - RESOLUTION OF ANGLE OF ATTACK

Angle of attack (α)	X Component	Y Component
0°	1.0000	0.0000
-2°	0.9993	-0.0348
-4°	0.9975	-0.0697
-6°	0.9945	-0.1045

The solution was initialized from the pressure far field and the calculation was run until the point a convergence was reached in the residual plot plotted for various parameters like X-velocity, Y-velocity, turbulence kinetic energy (k) and turbulence dissipation rate (ε).

C. Post - Processing

1) Pathlines

Pathlines (or vectors) represent the flow direction and the path of the fluid upon its interaction with the Gurney flap in the trailing edge of the airfoil. The Pathlines are colored by a velocity magnitude from 0 m/s to 60 m/s, such that the inlet condition of 33 m/s is satisfied. They are released from the pressure far field and leave through the outlet.

The pathline visualization for a velocity magnitude of 0 m/s to 60 m/s for different Gurney heights (H_g) for an angle of attack (α) of 0° are represented below.

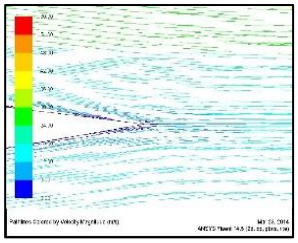

(a) Gurney Height (H_g) = 0.0%

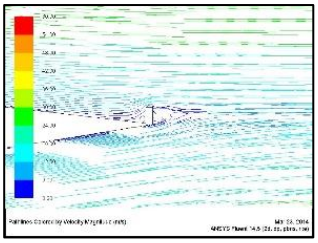

(b) Gurney Height (H_g) = 0.5%

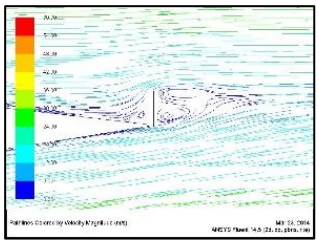

(c) Gurney Height (H_g) = 1.0%

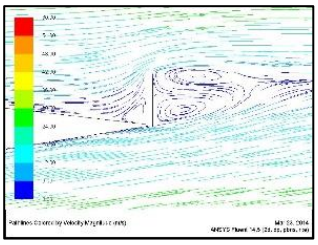

(d) Gurney Height (H_g) = 1.5%

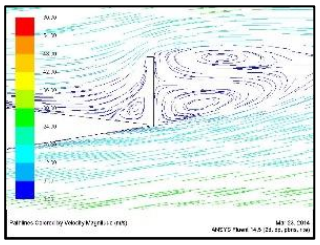

(e) Gurney Height (H_g) = 2.0%

Figure 13 - Velocity magnitude (0 m/s to 60 m/s) for α = 0°

The pathline visualization for a velocity magnitude of 0 m/s to 60 m/s for different Gurney heights (H_g) for an angle of attack (α) of -2° are represented below.

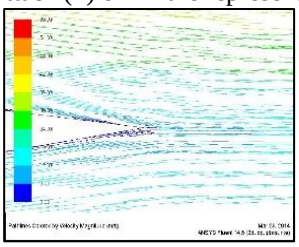

(a) Gurney Height (H_g) = 0.0%

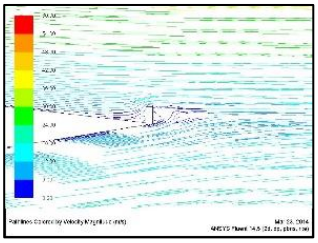

(b) Gurney Height (H_g) = 0.5%

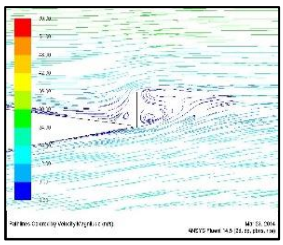

(c) Gurney Height (H_g) = 1.0%

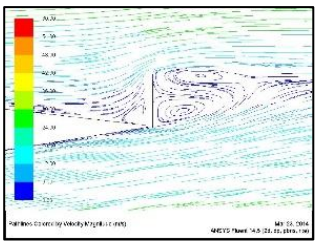

(d) Gurney Height (H_g) = 1.5%

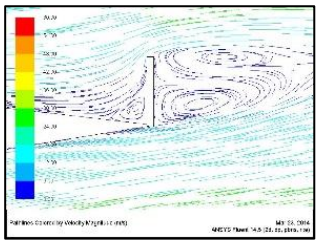

(e) Gurney Height (H_g) = 2.0%

Figure 14 - Velocity magnitude (0-60 m/s) for α = -2°

International Journal of Engineering Research & Technology (IJERT)
ISSN: 2278-0181
Vol. 8 Issue 05, May-2019

The pathline visualization for a velocity magnitude of 0 m/s to 60 m/s for different Gurney heights (H_g) for an angle of attack (α) of -4° are represented below.

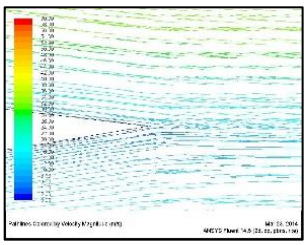

(a) Gurney Height (H_g) = 0.0%

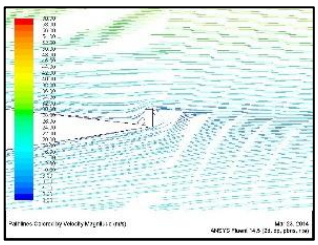

(b) Gurney Height (H_g) = 0.5%

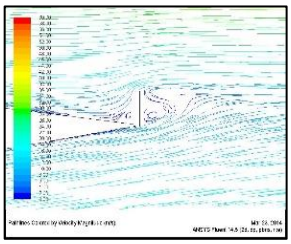

(c) Gurney Height (H_g) = 1.0%

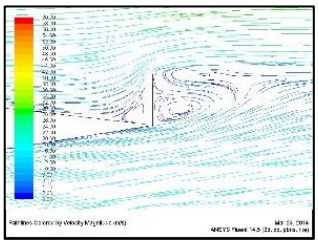

(d) Gurney Height (H_g) = 1.5%

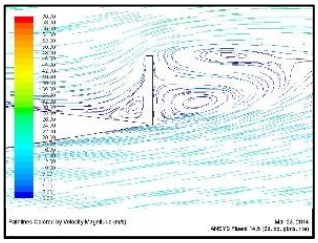

(e) Gurney Height (H_g) = 2.0%

Figure 15 - Velocity magnitude (0-60 m/s) for α = -4°

The pathline visualization for a velocity magnitude of 0 m/s to 60 m/s for different Gurney heights (H_g) for an angle of attack (α) of -6° are represented below.

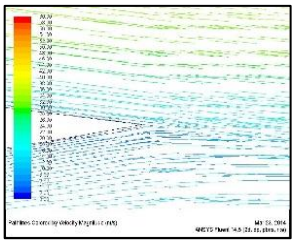

(a) Gurney Height (H_g) = 0.0%

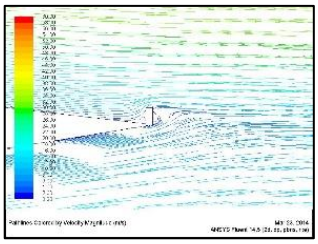

(b) Gurney Height (H_g) = 0.5%

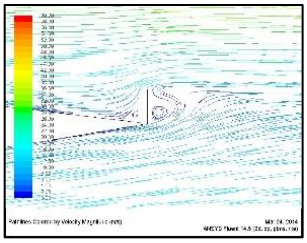

(c) Gurney Height (H_g) = 1.0%

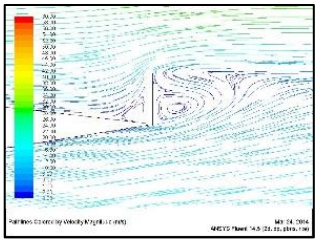

(d) Gurney Height (H_g) = 1.5%

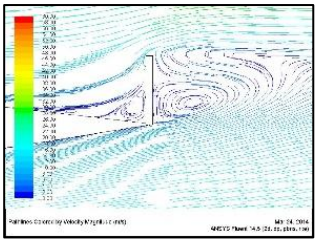

(e) Gurney Height (H_g) = 2.0%

Figure 16 - Velocity magnitude (0-60 m/s) for α = -6°

From the pathlines, it was inferred that the vortices formed at the trailing edge of the airfoil conforms to the Karman Vortex condition. Thus creating a high-pressure region near the Gurney flap and makes the flow remain attached to the airfoil surface, thus delaying the flow separation.

2) Contours of Pressure Coefficient

The contours of pressure coefficient show how the pressure is distributed around the airfoil. The pressure contours on the lower surface of the airfoil are minimal in comparison to the upper surface, which means that more downforce is exerted on the rear wing.

The contours of pressure coefficient for various Gurney heights (H_g) for an angle of attack (α) of 0° are represented below.

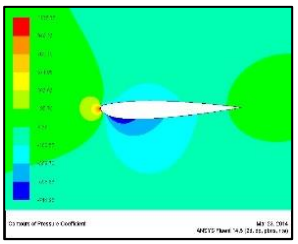

(a) Gurney Height (H_g) = 0.0%

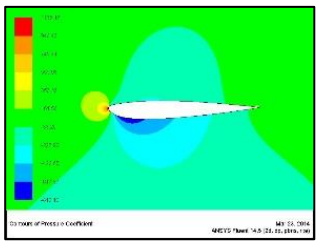

(b) Gurney Height (H_g) = 0.5%

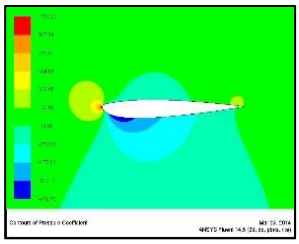

(c) Gurney Height (H_g) = 1.0%

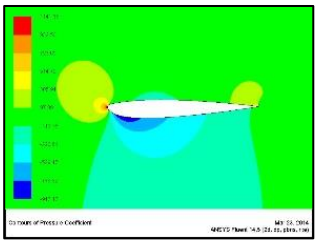

(d) Gurney Height (H_g) = 1.5%

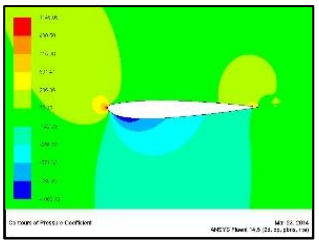

(e) Gurney Height (H_g) = 2.0%

Figure 17 - Contours of pressure coefficient for α = 0°

The contours of pressure coefficient for various Gurney heights (H_g) for an angle of attack (α) of -2° are represented below.

International Journal of Engineering Research & Technology (IJERT)
ISSN: 2278-0181
Vol. 8 Issue 05, May-2019

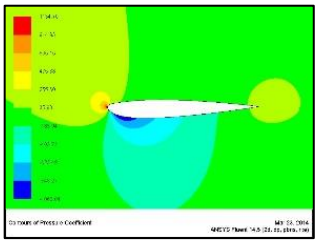

(a) Gurney Height (H_g) = 0.0%

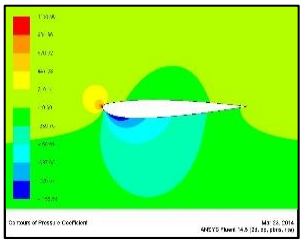

(b) Gurney Height (H_g) = 0.5%

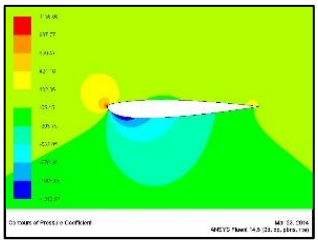

(c) Gurney Height (H_g) = 1.0%

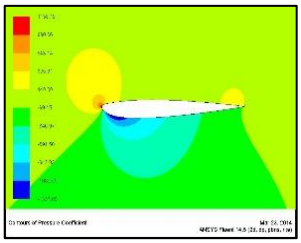

(d) Gurney Height (H_g) = 1.5%

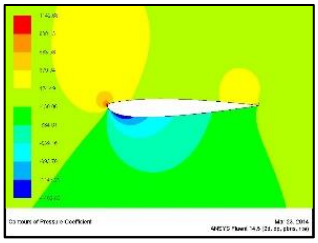

(e) Gurney Height (H_g) = 2.0%

Figure 18 - Contours of pressure coefficient for α = -2°

The contours of pressure coefficient for various Gurney heights (H_g) for an angle of attack (α) of -4° are represented below.

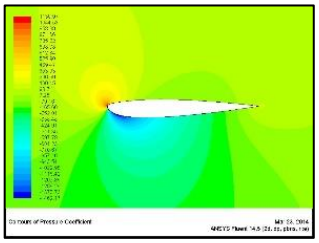

(a) Gurney Height (H_g) = 0.0%

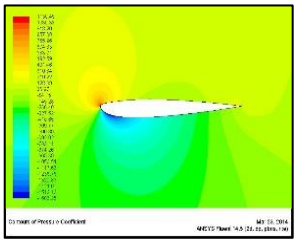

(b) Gurney Height (H_g) = 0.5%

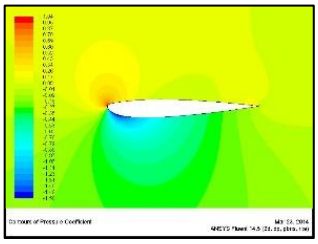

(c) Gurney Height (H_g) = 1.0%

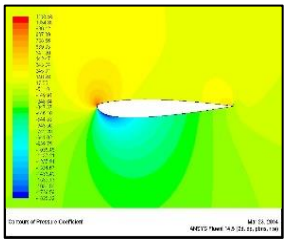

(d) Gurney Height (H_g) = 1.5%

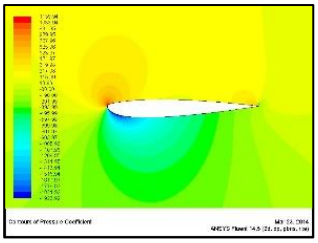

(e) Gurney Height (H_g) = 2.0%

Figure 19 - Contours of pressure coefficient for α = -4°

The contours of pressure coefficient for various Gurney heights (H_g) for an angle of attack (α) of -6° are represented below.

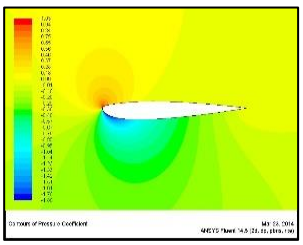

(a) Gurney Height (H_g) = 0.0%

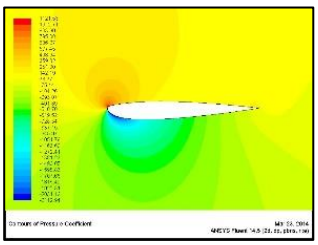

(b) Gurney Height (H_g) = 0.5%

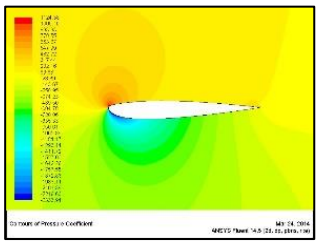

(c) Gurney Height (H_g) = 1.0%

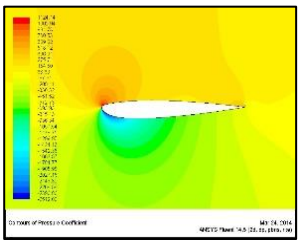

(d) Gurney Height (H_g) = 1.5%

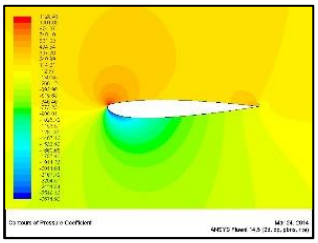

(e) Gurney Height (H_g) = 2.0%

Figure 20 - Contours of pressure coefficient for α = -6°

It was deduced from the contours of pressure coefficient plot that the pressure distribution at the top surface of the airfoil increases slowly as the angle of attack increases. It was also noted that the stagnation point moves towards the trailing edge on the upper surface as the angle of attack increases.

3) Pressure Coefficient Plot

The pressure coefficient plot gives the value of the pressure coefficient at the top surface, bottom surface and at the Gurney of the rear wing. It is the statistical representation of the contours of pressure coefficient in a graphical format from which results can be inferred easily.

The coefficient of plot for the different Gurney Heights (H_g) for an angle of attack (α) of 0° are visualized below.

International Journal of Engineering Research & Technology (IJERT)
ISSN: 2278-0181
Vol. 8 Issue 05, May-2019

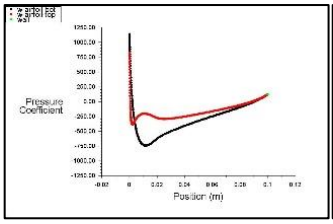
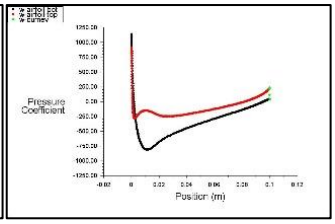

(a) Gurney Height (H_g) = 0.0% (b) Gurney Height (H_g) = 0.5%

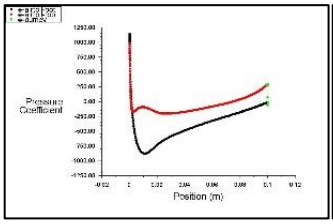
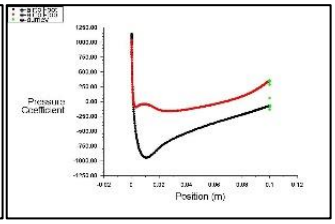

(c) Gurney Height (H_g) = 1.0% (d) Gurney Height (H_g) = 1.5%

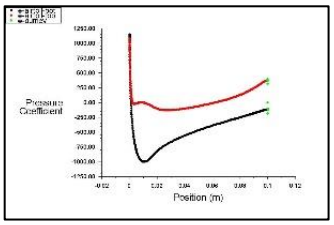

(e) Gurney Height (H_g) = 2.0%

Figure 21 - Pressure Coefficient plot for α = 0°

The coefficient of plot for the different Gurney Heights (H_g) for an angle of attack (α) of -2° are visualized below.

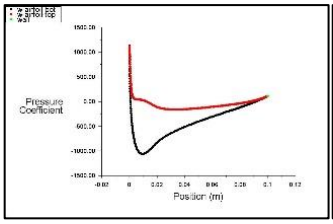
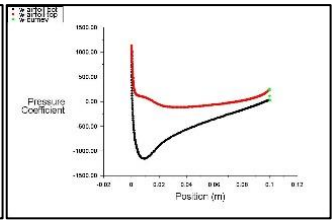

(a) Gurney Height (H_g) = 0.0% (b) Gurney Height (H_g) = 0.5%

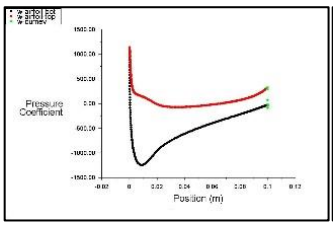
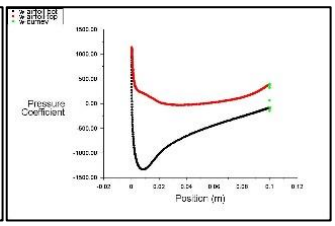

(c) Gurney Height (H_g) = 1.0% (d) Gurney Height (H_g) = 1.5%

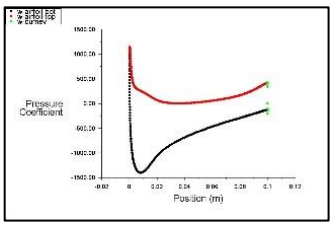

(e) Gurney Height (H_g) = 2.0%

Figure 22 - Pressure Coefficient plot for α = -2°

The coefficient of plot for the different Gurney Heights (H_g) for an angle of attack (α) of -4° are visualized below.

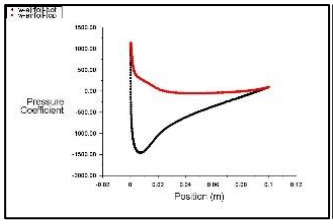
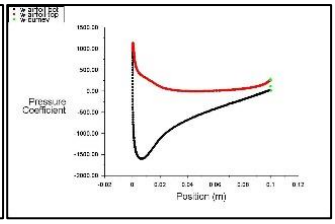

(a) Gurney Height (H_g) = 0.0% (b) Gurney Height (H_g) = 0.5%

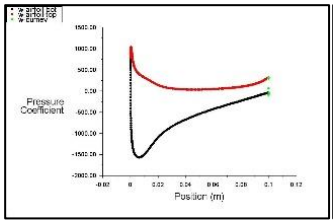
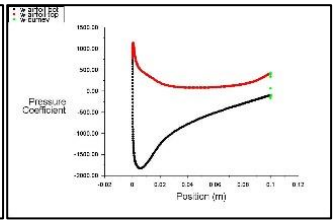

(c) Gurney Height (H_g) = 1.0% (d) Gurney Height (H_g) = 1.5%

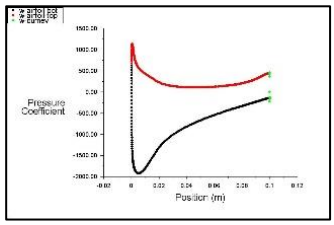

(e) Gurney Height (H_g) = 2.0%

Figure 23 - Pressure Coefficient plot for α = -4°

The coefficient of plot for the different Gurney Heights (H_g) for an angle of attack (α) of -6° are visualized below.

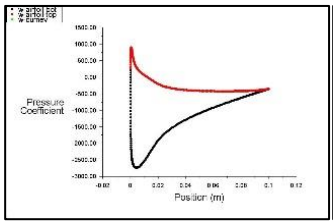
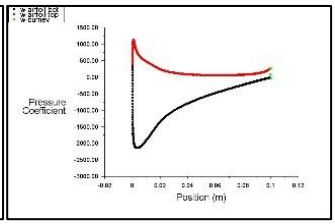

(a) Gurney Height (H_g) = 0.0% (b) Gurney Height (H_g) = 0.5%

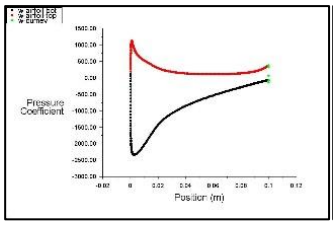
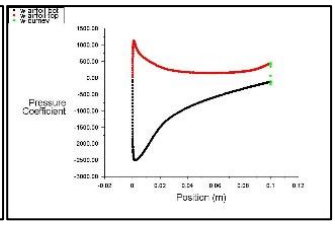

(c) Gurney Height (H_g) = 1.0% (d) Gurney Height (H_g) = 1.5%

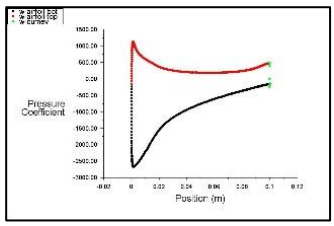

(e) Gurney Height (H_g) = 2.0%

Figure 24 - Pressure Coefficient plot for α = -6°

From the pressure coefficient plot, it was noted that the plot lines representing the upper surface of the airfoil is greater

International Journal of Engineering Research & Technology (IJERT)
ISSN: 2278-0181
Vol. 8 Issue 05, May-2019

than the one representing the lower line. Therefore, it can be inferred that the rear wing experiences sufficient downforce.

VII. RESULTS AND DISCUSSIONS

A. *Downforce Plot*

Downforce is the measure of force acting on the rear wing that is required to adhere the automobile to the ground. The downforce generated in the airfoil was plotted for various heights of Gurney and various angles of attack. The downforce data obtained from ANSYS Fluent was in the form of a negative lift. The original sign convention was changed from negative to positive to maintain consistency of upward flowing curves.

TABLE 3 - DOWNFORCE GENERATED FOR VARIOUS GURNEY HEIGHTS AND ANGLE OF ATTACK

H_g Vs α	0%	0.5%	1%	1.5%	2%
0º	08.50	14.61	20.75	26.66	31.24
-2º	22.65	29.87	36.52	43.14	47.80
-4º	37.13	45.76	52.73	59.27	64.51
-6º	50.86	59.83	67.86	74.48	80.00

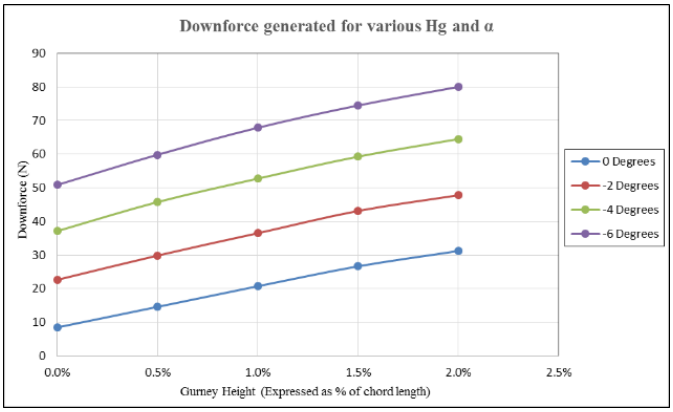

Figure 25 - Downforce generated for the various Gurney heights (H_g) for the various angles of attack (α)

B. *Drag Plot*

Drag is the force that gives resistance and acts in the opposite direction to the airflow. It hinders the aerodynamics of the rear wing and has to be as minimum as possible. Though drag cannot be eliminated, it can be minimized to a particular extent. The drag produced in the rear wing was plotted for the variation of height of Gurney and the variation of angles of attack.

TABLE 4 - DRAG FORCE GENERATED FOR VARIOUS GURNEY HEIGHTS AND ANGLE OF ATTACK

H_g Vs α	0%	0.5%	1%	1.5%	2%
0º	1.72	1.74	1.84	1.91	2.06
-2º	1.83	1.90	2.04	2.15	2.33
-4º	2.04	2.15	2.34	2.51	2.70
-6º	2.39	2.60	2.80	3.04	3.24

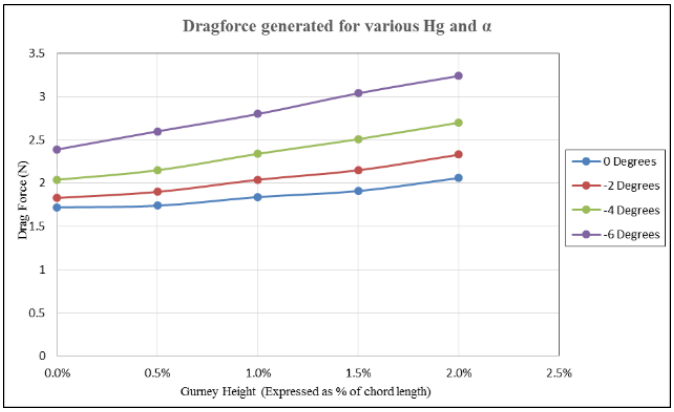

Figure 26 - Drag force generated for the various Gurney heights (H_g) for the various angles of attack (α)

C. *Downforce to Drag Ratio (L/D) Plot*

The downforce to drag (L/D) ratio plot helps us to arrive at the trade-off point between the generated downforce and the experienced drag force. The best optimum point of the Gurney was obtained by comparing the slope of the plot.

TABLE 5 - DOWNFORCE TO DRAG FORCE RATIO (L/D) GENERATED FOR VARIOUS GURNEY HEIGHTS AND ANGLE OF ATTACK

Hg Vs α	0%	0.5%	1%	1.5%	2%
0º	04.93	08.37	11.27	13.93	15.11
-2º	12.37	15.66	17.89	20.02	20.48
-4º	18.19	21.19	22.51	23.56	23.80
-6º	21.26	22.96	24.20	24.46	24.63

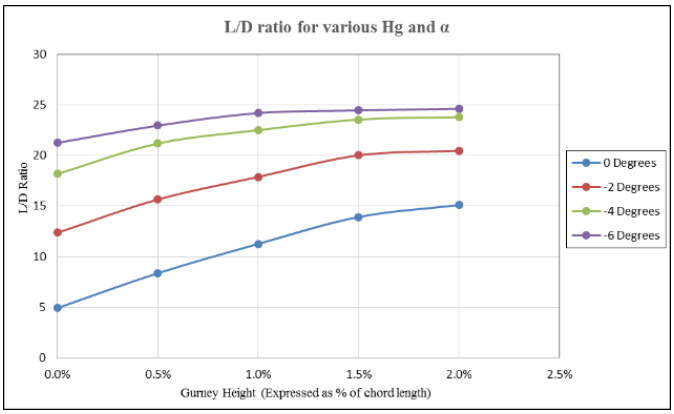

Figure 27 - Downforce generated to drag force ratio (L/D ratio) for the various Gurney heights (H_g) for the various angles of attack (α)

The downforce to drag (L/D) ratio values plotted revealed that it increases with an increase in the angle of attack (α), as with an increase in the height of the Gurney Flap (H_g). It was noted that the slope of the increasing trend in the L/D ratio graph decreases with an increase in the Gurney height. From the L/D ratio Vs. Gurney height, it was noted that the maximum L/D ratio occurs for a Gurney height of 1% and remains almost a constant for both 1.5% and 2%. From the above analyses, it was deduced that the optimal values for the Gurney height is 1% of the chord length for an angle of attack -6º.

International Journal of Engineering Research & Technology (IJERT)
ISSN: 2278-0181
Vol. 8 Issue 05, May-2019

VIII. CONCLUSION

With tremendous growth in technologies and several advancements in the automotive industries concerning aerodynamics application, the study of flow phenomenon plays a major role in understanding the fluid - wall interactions, not only at the rear wing but also in the vehicle as a whole. In addition, innovations that are more so often frugal are required for taking the technology forward and many OEMs are investing trillions of dollars to foray into advancements through research and development. As to optimize the performance of a rear wing without altering its design and with minimum investment, this research paper serves as a perfect example for such a frugal innovation. So as to the future scope of furthering the research in this field, the Gurney flap can be analyzed considering the ground effect into place, as this may influence the fluid flow parameters around the rear wing. In addition, a stepped airfoil design can be used in conjunction with the Gurney flap to analyze its effects on the overall performance of the rear wing.

REFERENCES

[1] https://en.wikipedia.org/wiki/Airfoil

[2] https://allamericanracers.com/the-Gurney-flap

[3] http://www.aviation-history.com/theory/airfoil.htm

[4] Greg F Altmann (2011), 'An Investigative Study of Gurney Flaps on a NACA 0036 Airfoil' - California Polytechnic State University.

[5] Michael A. Cavanaugh, Paul Robertson, William H. Mason (2007), 'Wind Tunnel Test of Gurney Flaps and T-Strips on an NACA 23012 Wing' - AIAA Journal 4175.

[6] Yoo, NS. KSME International Journal (2000) 14: 1013. https://doi.org/10.1007/BF03185804

[7] Shubham Jain, Nekkanti Sitaram and Sriram Krishnaswamy (2005), 'Computational Investigations on the Effects of Gurney Flap on Airfoil Aerodynamics' - ISRN Journal, 402358